Iraqi Journal of Physics, 2026
https://doi.org/10.30723/ijp.v24i3.1456

Vol.24, No.3, PP.125-135
P-ISSN: 2070-4003
E-ISSN: 2664-5548

Optical and Structural Properties of TFB:Graphene Thin Films Prepared by the Spin Coating Technique

Sujood B. Jabr[1*] and Raied K. Jamal[1]
[1]*Department of Physics, College of Science, University of Baghdad, Baghdad, Iraq*
[*]Corresponding author: sijood.bassem1604a@sc.uobaghdad.edu.iq

Abstract

In this work, the structural and optical properties of graphene (Gr), poly(9,9-dioctylfluorene-alt-N-(4-sec-butylphenyl)-diphenylamine) (TFB) polymer, and TFB:Gr composite thin films prepared by spin coating were investigated. The films were deposited on glass substrates at a rotational speed of 1000 rpm for 16 s and subsequently annealed at 60 °C for 30 min. TFB:Gr composite solutions with volume ratios of 5:1, 5:2, 5:3, 5:4, and 5:5 were examined to determine the influence of Gr content on the film properties. X-ray diffraction (XRD) analysis showed that the 5:3 sample exhibited a distinct peak at 2θ = 26.543°, indicating the presence of the Gr structure. Optical absorption measurements revealed that increasing the Gr ratio resulted in a decrease in the energy gap from 3 to 2.91 eV. The fluorescence spectra also showed systematic changes in peak intensity, accompanied by luminescence quenching after incorporating Gr into the TFB matrix. These results demonstrate that controlling the TFB:Gr mixing ratio provides an effective approach for tuning the structural and optical properties of the composite thin film.

Article Info.

Keywords:
Semiconductor, Polymers, Optical Properties, Structural Properties, Spin Coating.

Article history:
Received:Mar. 22, 2025
Revised: Jul. 19, 2025
Accepted: Jul. 25, 2025
Published:Sep. 01,2026

1. Introduction

Given the importance of graphene (Gr) in industrial and optical applications and its outstanding electronic and electrical properties, its integration with organic polymers such as poly(9,9-dioctylfluorene-alt-N-(4-sec-butylphenyl)-diphenylamine) (TFB) is a promising step toward producing improved hybrid films. The Gr is characterized by unique properties, such as its atomic thickness, high electrical conductivity, and chemical stability, which make it ideal for detecting a wide range of materials [1-8]. Gas sensor manufacturing techniques have recently developed through the use of various materials and techniques. The Gr can be used in gas sensors due to its ability to quickly interact with different gas molecules [9-13]. On the other hand, TFB polymer is considered one of the materials that have distinctive optical, structural, and electrical properties that make it suitable for use in organic electronic applications [13-14]. TFB polymer is characterized by high light absorption in the near-ultraviolet and visible region, which makes it suitable for use in organic lighting devices and other electronic devices that depend on interaction with light. Studies are also currently being conducted on its use as a promising gas sensor, as it is considered an effective material due to its high potential to improve the properties of sensors, as it is characterized by the ability to be chemically modified or combined with other materials. However, challenges related to stability and selectivity must be overcome to achieve maximum benefit from it in practical applications [15-16]. This study aims to explore the relative influence of Gr in TFB polymers on yield and optical structure, and hypothesize that an optimal ratio exists that helps minimize optical absorption and surface roughness. The study was supported by multiple analytical techniques, such as XRD, UV-Vis, PL, and AFM.

2. Experimental Work

Independent samples were prepared for different mixing ratios of TFB and Gr. Spin-coating was used at 1000 rpm for 16 seconds, followed by a heat treatment at 60°C for 30

minutes. These conditions were selected based on preliminary experiments and published studies confirming their effectiveness in producing homogeneous thin films [17].

2.1. Preparation of TFB Polymer

0.06 g of TFB polymer (purchased from American Dye Source, Inc.) was completely dissolved in 4 mL of chloroform. To obtain thin films, the resulting solution was applied using a spin-coating technique to a glass substrate after being cleaned. The thin films were then placed in a thermal oven for 30 minutes at 60 ^{o}C.

2.2. Graphene Preparation

0.25 g of Gr was dissolved in 4 mL of chloroform solution and then placed on a magnetic stirrer at room temperature for 1 h to obtain a well-mixed solution. The solution was deposited on a glass substrate using the spin coating technique at a speed of 1000 rpm for 16 s to obtain thin films. The glass substrates were then placed in a thermal oven at a temperature of 60 ^{o}C for 30 min.

2.3. Preparation of TFB:Gr Thin Films

TFB polymer solution was mixed with five different volume ratios of Gr (TFB:Gr 5:1, 5:2, 5:3, 5:4, 5:5), then deposited on a glass substrate by the spin-coating technique for 16 s at a speed of 1000 rpm and then placed in a thermal oven at a temperature of 60 ^{o}C for 30 min. After completing the thin film preparation process, the optical and structural properties of the thin films were studied before and after mixing using UV-Vis. After preparing the thin films, their optical and structural properties before and after mixing were studied using UV-Vis, photoluminescence (PL), AFM, and XRD techniques.

3. Results and Discussion

3.1. Structural Properties

The structural properties of TFB polymer, Gr, and TFB:Gr were studied using XRD. Gr XRD pattern shown in Fig. 1 showed several peaks at 2θ of 26^{o}, 54^{o}, and 77 °, corresponding to Miller indices (hkl) of (002), (004), and (110), with a distinctive peak at 2θ equal to 26.543. The results indicated a polycrystalline structure. When comparing the peaks obtained with the standard card ID (96-901-1578), it was found that the resulting structure is hexagonal. The Scherrer eq. was applied to calculate the crystallite size (D) of the resulting structure [17]:

$$D = \frac{k\lambda}{\beta \cos\theta} \quad (\mathbf{1})$$

where K, λ, β, and θ represent the dimensionless form factor with a value of 0.9, the X-ray wavelength, the line broadening at half the maximum intensity (FWHM) measured in radians, and the Bragg angle measured in degrees, respectively. It was found that the crystal size of the distinctive peak equals 11 nm. Table 1 shows most of the structural values obtained through the XRD pattern, which is consistent with the results of Xu et al. [18]. The XRD pattern of TFB polymer shown in Fig. 2 shows that the resulting structure is amorphous. This result is in agreement with that of Campbell et al. [19]. The TFB:Gr XRD pattern at the ratio of 5:3 showed a single distinct peak due to the Gr structure at 2θ = 26.543 °, as shown in Fig. 3 and Table 1.

Figs. 4-8 show the AFM images of TFB:Gr thin films (prepared at different mixing ratios), from which the structure and surface morphology of the thin films were studied. The images revealed that the average grain size decreased with increasing Gr content, except for

the 5:2 ratio. Conversely, the average roughness increased with increasing Gr concentration, peaking at 4.217 for the 5:3 ratio and reaching a minimum of 1.99 at the 5:4 ratio, as detailed in Table 2. This is due to the physical nature of Gr, the effect of non-degradable distribution, interactions between Gr and TFB, the effect of layer thickness, and the preparation and deposition methods. This behavior can be modified by controlling the rotation speed or heat treatment to optimize the system. By analyzing the histograms of the grain size distribution of the prepared films, the films at the ratios 5:4 and 5:5 show a regular distribution, as shown in Figs. 7 and 8.

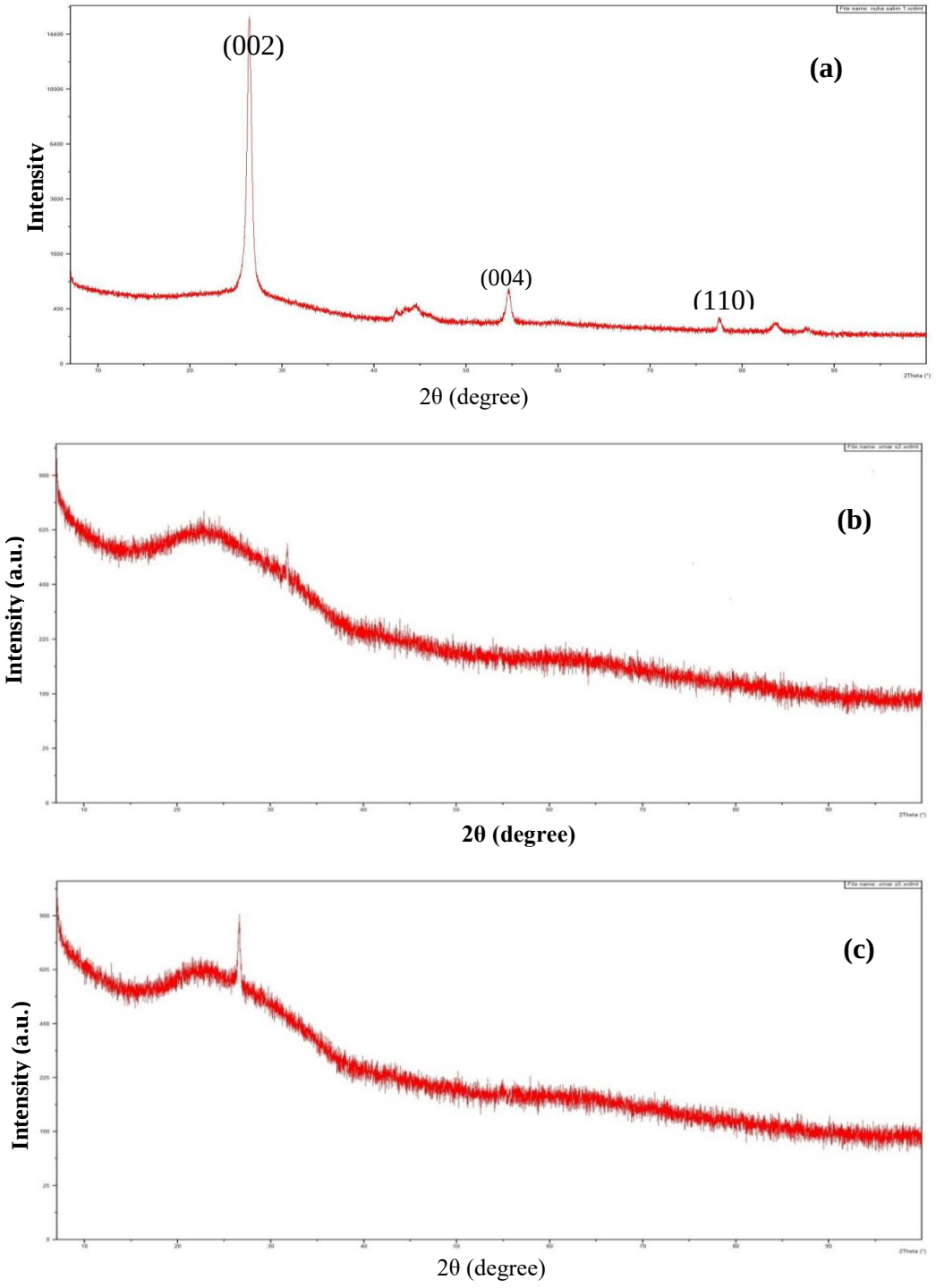

Figure 1: XRD of (a) pure Gr,(b) pure TFB Polymer and (c) TFB:Gr at a ratio 5:3 at 1μm.

Table1: XRD information of Gr and 5:3 thin film.

Samples	Peak No.	2θ(degree)	FWHM(degree)	d(A)	(hkl)	G(nm)
Gr	1	26.543	0.228	3.355	(002)	36.47
	2	54.661	0.382	1.677	(004)	24.79
	3	77.400	0.615	1.232	(110)	16.69
5:3	1	26.642	0.261	3.343	(1 0-1)	31.35

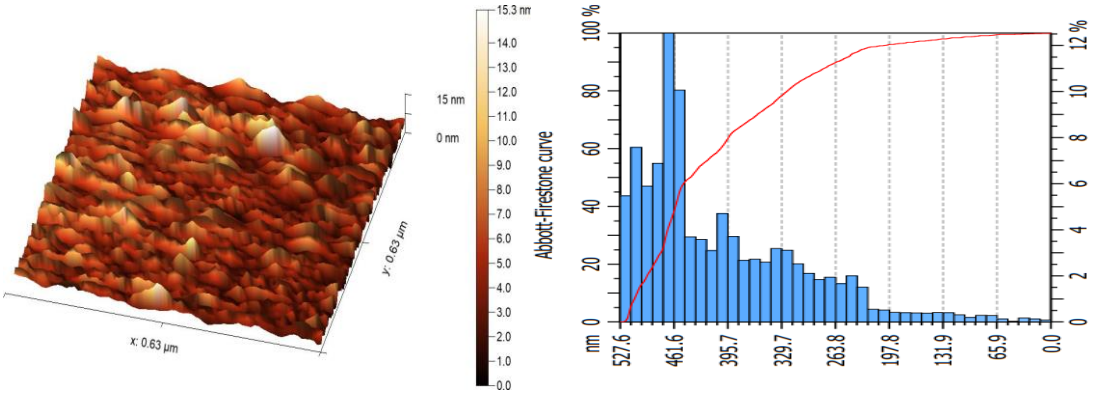

Figure 4: AFM of TFB:Gr at 5:1 ratio.

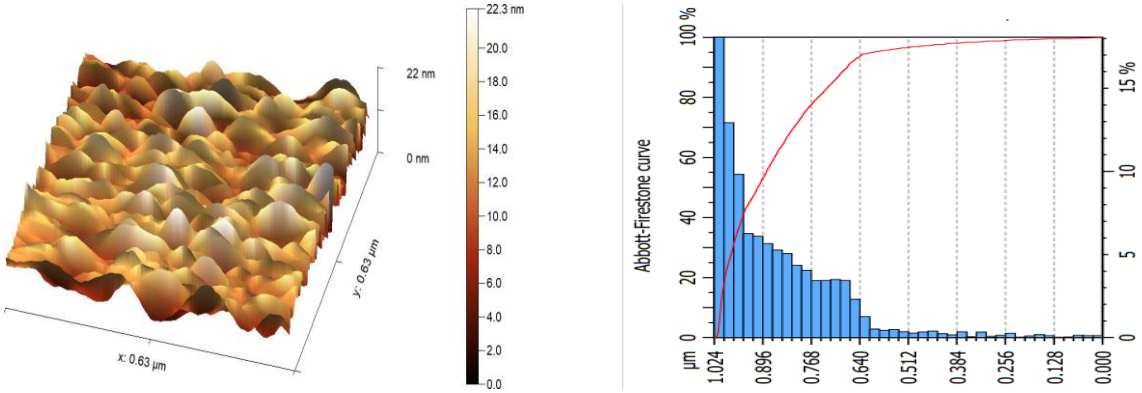

Figure 5: AFM of TFB: G at 5:2 ratio.

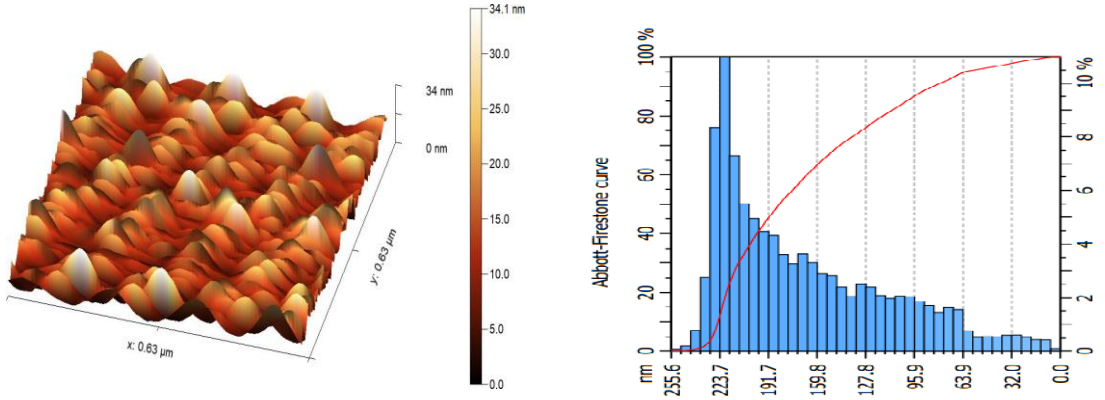

Figure 6: AFM of TFB:Gr at 5:3 ratio.

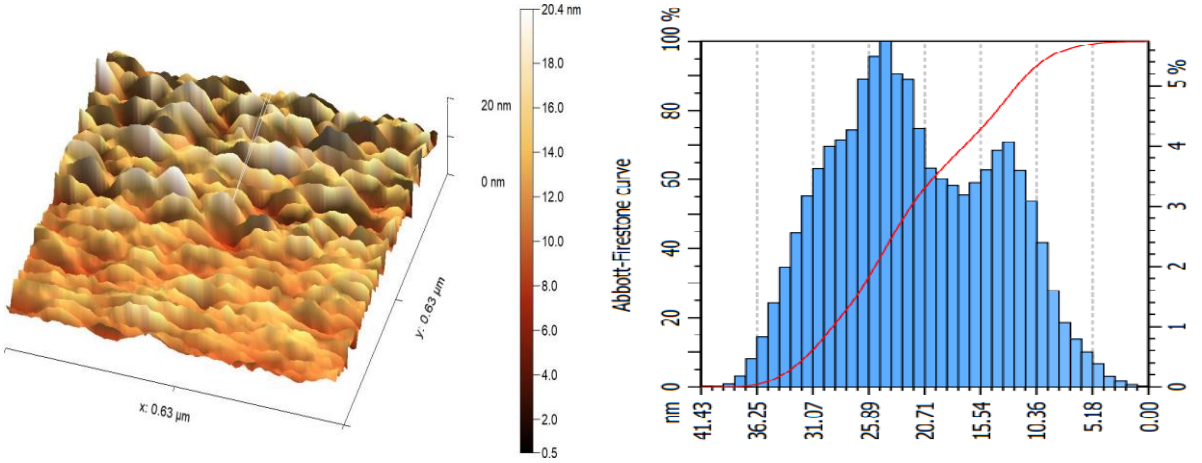

Figure 7: AFM of TFB:Gr at 5:4 ratio.

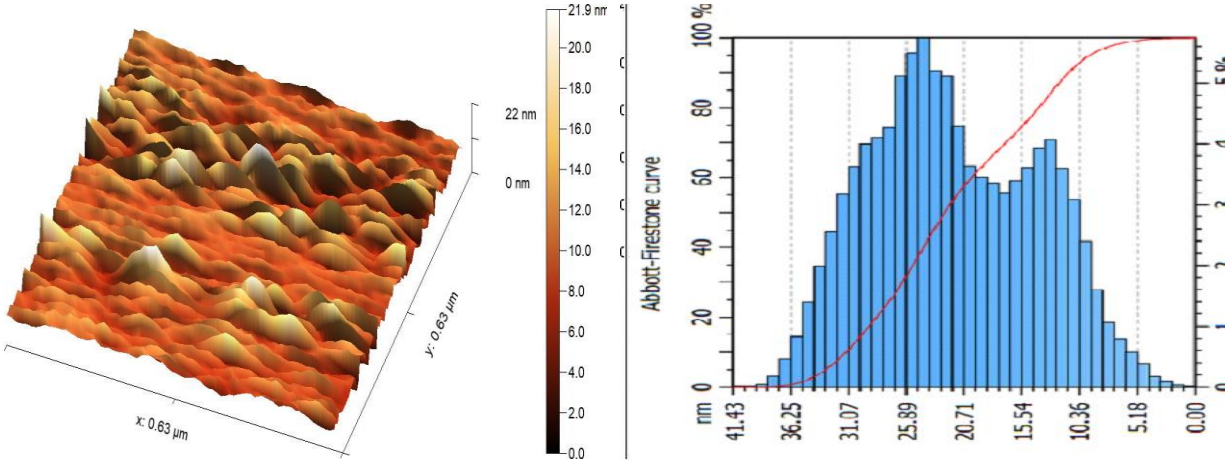

Figure 8: AFM of TFB:Gr at 5:5 ratio.

Table 2: AFM characteristics of TFB:Gr at different ratios.

Mixing ratio TFB:Gr	Average value (nm)	RMS roughness (Sq) (nm)	RMS (nm)	Mean roughness (Sa) (nm)
5:1	28.7268	3.03573	3.03573	2.37436
5:2	42.3734	3.92810	3.92810	2.85372
5:3	17.9634	5.35567	5.35567	4.21717
5:4	10.7333	2.50393	2.50393	1.99524
5:5	9.8464	2.54358	2.54358	2.03052

3.2. Optical Properties

The optical properties of all prepared thin films with a thickness of 1 µm were studied in the range of 300-800 nm, as shown in Fig. 9. The results showed that the maximum absorption of Gr starts at 339 and extends to 800 nm, which is consistent with other studies [21-22]. Gr absorbs approximately 2.3% of incident light across a wide wavelength range, from visible (400–700 nm) to infrared. This 2.3% ratio is equivalent to πα (where α is the fine-structure constant ≈ 1/137), a characteristic feature resulting from Gr's electronic structure. In the ultraviolet region (<400 nm), Gr's absorption increases significantly due to

electron transitions from the valence band to the higher conduction band. Applying the Tauc equation for the direct transition [22], the energy gap value was equal to 1.1 eV, as shown in Fig. 10. The absorption spectrum results of the 1 μm-thick TFB polymer thin film showed an absorption peak at a wavelength of 379 nm, as shown in Fig. 9. The width of this peak lies in the range of 300-430 nm, while the energy gap value for these thin films is equal to 3 eV, as shown in Fig. 10.

To study the effect of adding Gr to TFB polymer in different ratios on its optical properties and energy gap, it was found that the higher the Gr ratio, the more the absorption peak shifts towards the short wavelength (blue shift) [23], as is clear in Fig. 9. The energy gap of the mixture decreased as the Gr ratio increased, where the energy gap value at the 5:1 ratio was 2.98 eV and became 2.91 eV at the 5:5 ratio, as evident from Fig. 10. Table 3 lists the optical properties of pure Gr, TFB polymer, and the five ratios of the TFB:Gr mixture. These results agree with many reported studies [24-27].

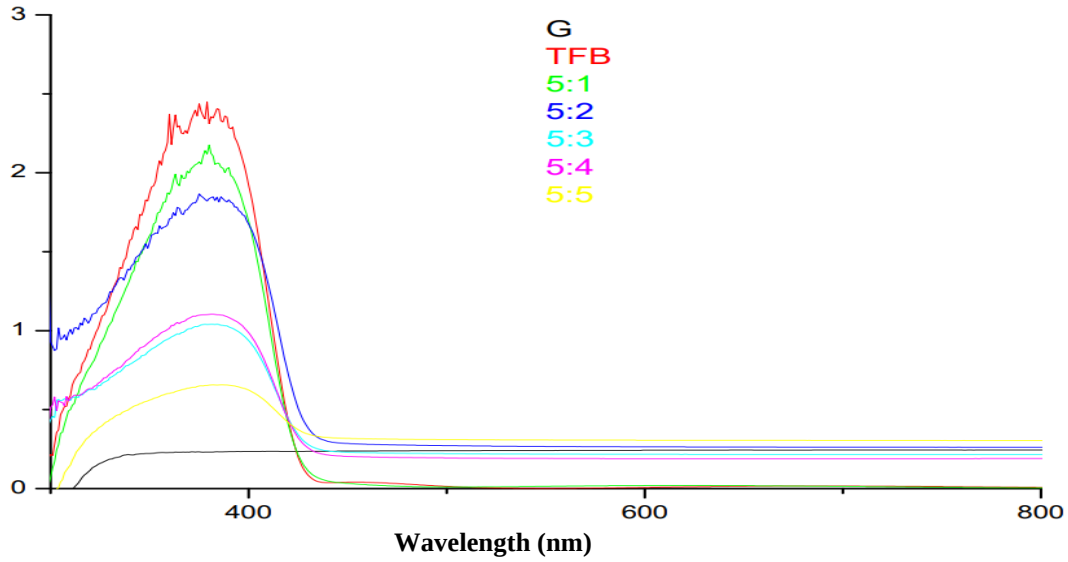

Figure 9: UV-Vis spectrum of graphene, TFB, and the different ratios of TFB:Gr.

The fluorescence spectra of both pure Gr and TFB polymer were studied and analyzed, in addition to evaluating the effect of adding Gr at different ratios to TFB polymer. The spectra were measured using different excitation wavelengths, as shown in Fig. 11 and Table 4, with the aim of understanding the changes in fluorescence intensity and emission sites resulting from the interaction between Gr and the polymer and the effect of different concentrations on the optical properties of the materials. The fluorescence spectrum of Gr showed a distinct peak at 407 nm using an excitation wavelength of 372 nm, while the photoluminescence (PL) spectrum of TFB polymer showed a distinct peak at 434 nm using an excitation wavelength of 363 nm.

The reason for choosing this wavelength is the strong absorption at 363 nm due to π–π* transitions in the fluorine ring of the polymer. The explanation for the occurrence of a distinct peak in the emission spectrum of the Gr polymer and TFB that differs from the excitation wavelength is the loss of a portion of the energy in the form of internal vibrations (relaxation), a phenomenon called the Stokes effect.

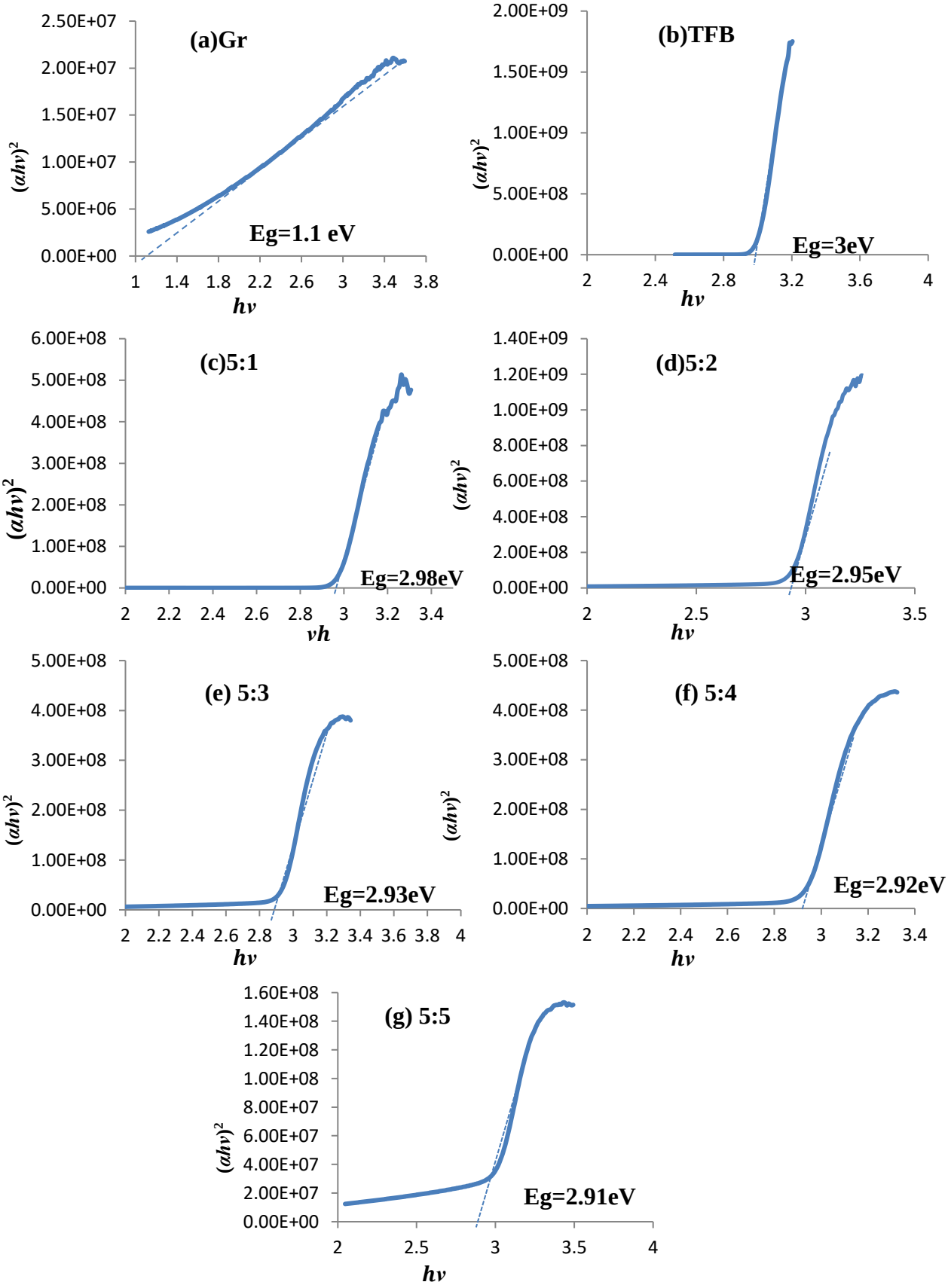

Figure 10: Tauc plot of (a)Gr, (b)TFB, (c)5:1, (d)5:2, (e)5:3, (f)5:4, and (g)5:5 ratios.

Table 3: The optical properties of Gr, pure TFB, and the TFB:Gr mixture.

TFB:Gr ratios	λpeak (nm)	Range (nm)	Eg (eV)
5:1	380	(300-500)	2.98
5:2	384	(300-431)	2.95
5:3	375	(300-431)	2.93
5:4	371	(300-431)	2.92
5:5	373	(300-431)	2.91
Pure G	300	(300-800)	1.1
Pure TFB	375	(300-428)	3

Mixing at different ratios produced several distinct peaks with decreasing intensity, as shown in Fig. 12 and Table 4. Gr is a highly effective fluorescence quencher because its electronic properties enable it to absorb fluorescence photons emitted by TFB. The appearance of multiple peaks in the fluorescence spectrum upon mixing is due to the influence of nanoscale and surface quantum states, which depend on the temperature of the molecules and the change in TFB polarity [28].

The improved optical results for the TFB:Gr films suggest that some kind of interaction may occur between the Gr layer and the TFB, which could lead to changes in the electronic or morphological structure of the film. However, the current study does not include spectroscopic analyses, such as Raman, FTIR, or XPS. Subsequent spectroscopic studies are recommended to verify the nature of the interaction and its impact on the properties of the produced films.

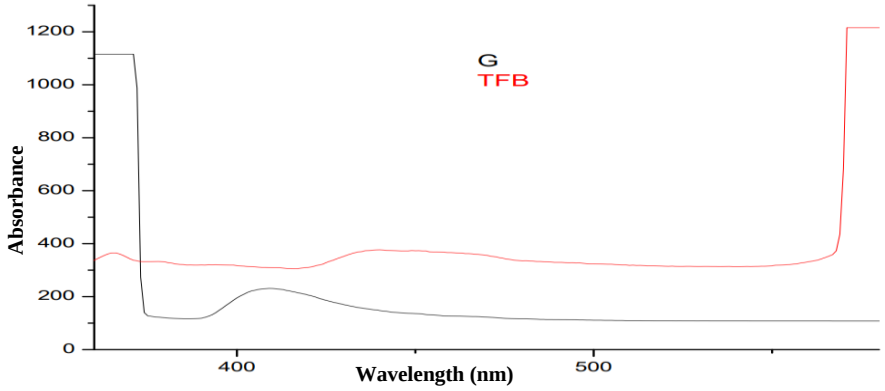

Figure 11: Photoluminescence of pure TFB polymer and Gr thin film.

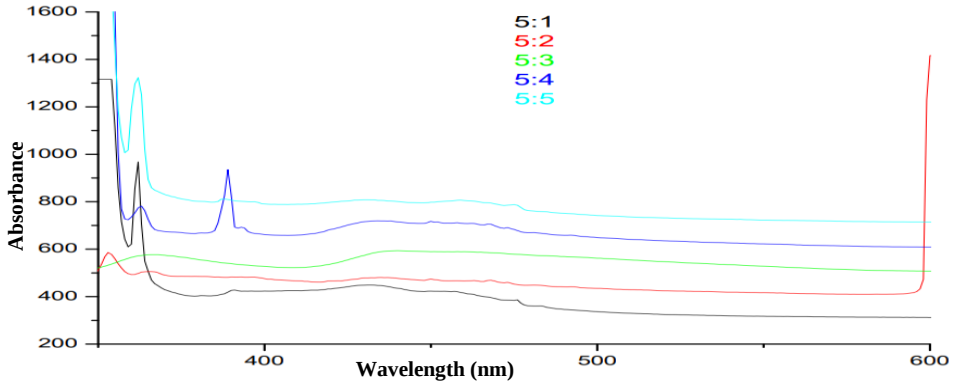

Figure 12: Photoluminescence of TFB:Gr thin film at different ratios.

Table 4: Excitation wavelengths and positions of characteristic fluorescence peaks for Gr and TFB and different mixing ratios.

Sample	λexc(nm)	λpl(nm)
Gr	372	407
TFB	363	434
5:1	362	429
5:2	337	357,363,432
5:3	363	435
5:4	363	389,431
5:5	361	427,458

4. Conclusions

In conclusion, the spin coating technique was a successfully employed to prepare TFB:Gr composite thin films with different mixing ratios. Structural analysis showed that incorporating Gr into the TFB matrix influenced the crystallite structure and reduced the calculated crystallite size. Optical analysis revealed a gradual decrease in the optical energy gap with increasing graphene content, demonstrating that the optical properties of the composite films can be tuned by controlling the TFB:Gr mixing ratio. The observed behavior may be associated with Gr-induced electronic states and interfacial interactions within the polymer matrix.

Conflict of Interest

The authors declare that they have no conflict of interest.

References

1. S. S. Varghese, S. Lonkar, K. K. Singh, S. Swaminathan, and A. Abdala, Recent advances in graphene based gas sensors, *Sens. and Actuators B: Chem.* **218**, 160 (2015). https://doi.org/10.1016/j.snb.2015.04.062.
2. Z. Chen, Q.Lei, Y. Ma, J. Wang, Y.Yan, J.Yin, J. Li, J.Shen, G. Li, T. Pan, X. Dong, B. Davaasuren, Y.Zhang, J.Z.Liu, J. Tao , Y.Han, Highly sensitive, responsive, and selective iodine gas sensor fabricated using AgI-functionalized graphene, *Nat. Commun.* **16,** 1169 (2025), https://doi.org/10.1038/s41467-025-56621-3.
3. A. S. Zamil and A. N. Naje, Preparation and characterization the physical properties of graphene/carbon nanotubes films, *J. Opt.* **53**, 3486 (2024). https://doi.org/10.1007/s12596-023-01481-7.
4. A. H. Mohammed, A. N. Naje, and R. K. Ibrahim, Photoconductive detector based on graphene doping with silver nanoparticles, *Iraqi J. Sci.* **63**(12), 5218 (2022). https://doi.org/10.24996/ijs.2022.63.12.12.
5. M. W. Kazem and R. K. Jamal, Characterization of copper phthalocyanine-tetrasulfonic acid tetrasodium salt /graphene oxide, *Iraqi J. Sci.* **62**(6), 1893 (2021). https://doi.org/10.24996/ijs.2021.62.6.15.
6. M. W. Kadhim and R. K. Jamal, Fabrication of a novel solar cell using copper phthalocyanine tetrasulfonic acid tetrasodium salt/graphene oxide. *J. Opt.* **52**, 1507 (2023). https://doi.org/10.1007/s12596-022-00960-7.
7. M. Ahmed, H. Ahmed, P. Adebayo, R. Carter, and L. Khanal, Mechanical properties and application of graphite and graphite-based nanocomposite: A Review, *Chem. Mater. Res.* **15**(1), (2023). https://doi.org/10.7176/CMR/15-1-02.
8. L. A. Abdullah, O. A. Ibrahim, and O. A. Ali, Determination of third order susceptibility of carbon quantum dots at different concentrations, *Mat. Lett.* **377**, 137534 (2024). https://doi.org/10.1016/j.matlet.2024.137534.
9. M. M. Faris and A. K. Ayal, Electrochemical synthesis of Fe-doped TiO_2 nanotube for gas sensor application, *Iraqi J. Sci.* **66**(4), 1437(2024). https://doi.org/10.24996/ijs.2025.66.4.4.
10. S. S. Al-Awadi, A. A Ramadhan, F. T. Ibrahim, and A. K. Abbood, Optical and structural properties of titanium dioxide papered by DC magneto-sputtering as a NO_2 Gas Sensor, *Iraqi J. Sci.* **61**(10), 2562 (2020). https://doi.org/10.24996/ijs.2020.61.10.12.
11. Tian W, Liu X, Yu W. Research Progress of Gas Sensor Based on Graphene and Its Derivatives: A Review. *App. Sci*. **8**(7), 1118 (2018). https://doi.org/10.3390/app8071118.

12. C. Cochrane, C. Hertleer, and A. Schwarz-Pfeiffer, Smart textiles in health: An overview, Woodhead Publishing Series in Textiles, 9-32 (2016). https://doi.org/10.1016/B978-0-08-100574-3.00002-3.
13. O. A. Ali and N. S. Sultan, Study of the sensitivity of carbon quantum dots for NO_2 gas sensor and improve it using Graphene, *Iraqi J. Phys.* **22**(4), 130 (2024). https://doi.org/10.30723/ijp.v22i4.1342.
14. W. Xu, et al., Rational molecular passivation for high-performance perovskite light-emitting diodes, *Nat. Photonics*. **13**(6), 1 (2019). https://doi.org/10.1038/s41566-019-0390-x.
15. M. -Y. Chuang, Y. -T. Lin, T. -W. Tung, L. -Y. Chang, H. -W. Zan, H. -F. Meng, C. -J. Lu, and Y.-T. Tao, Room-temperature-operated organic-based acetone gas sensor for breath analysis, *Sens. and Actuators B: Chem.* **260**, 593 (2018). https://doi.org/10.1016/j.snb.2017.12.168.
16. H. Min et al., Spin coating epitaxial heterodimensional tin perovskites for light-emitting diodes, Nat. *Nanotechnol*. **19**, 632 (2024). https://doi.org/10.1038/s41565-023-01588-9.
17. P. Scherrer, Nachrichten von der Gesellschaft der Wissenschaften zu Göttingen, Mathematisch-Physikalische Klasse. **2**, 98 (1918).
18. J. Xu, P. Krüge, R. Natoli, K. Hayakawa, Z. Wu, and K. Hatada, X-ray absorption spectra of graphene and graphene oxide by full-potential multiple scattering calculations with self-consistent charge density, *Phys. Rev. B.* **92**, 125408 (2015). https://doi.org/10.1103/PhysRevB.92.125408.
19. A. J. Campbell, R. Rawcliffe, A. Guite, J. C. D. Faria, A. Mukherjee, M. A. McLachlan, M. Shkunov, and D. D. C. Bradley, Charge-carrier density-independent mobility in amorphous fluorene-triarylamine copolymers. *Adv. Funct. Mater*. **26**, 3720 (2016). https://doi.org/10.1002/adfm.201504722.
20. E. K. Salman and G. S. Muhammed, Study of Some Structural and Optical Properties for Synthesized Graphene/Polyaniline/Zns Nanocomposite, *Iraqi J. Phys.* **22**(4), 53 (2024). https://doi.org/10.30723/ijp.v22i4.1244.
21. L. A. Falkovsky, Optical properties of graphene, *J. Phys.: Conf. Ser*. 129, 012004(2008). https://doi.org/10.1088/1742-6596/129/1/012004.
22. J. Tauc, Optical properties and electronic structure of amorphous Ge and Si, *Mater. Res. Bull.* **3**, 37 (1968). https://doi.org/10.1016/0025-5408(68)90023-8.
23. J. Yang, X. Zhao, X. Shan, H. Fan, L. Yang, Y. Zhang, and X. Li, Blue-shift of UV emission in ZnO/graphene composites, *J. Alloys Compd*. **556**, 1 (2013). https://doi.org/10.1016/j.jallcom.2012.12.098.
24. R. Nandee, M. A. Chowdhury, MD. A. Kowser, S. K. Nondy, N. Hossain, Md. Rasadujjaman, A. Al Mostazi, Md. B. Molla, S. Barua, Md. M. Rana, and Md. Sh. Islam, Bandgap formation in graphene doped with BN, TiO_2, Al_2O_3 and ZnO by sintering process, *Results Chem.* **6**, 101229 (2023).https://doi.org/10.1016/j.rechem.2023.101229.
25. R. Nandee, M. A. Chowdhury, A. Shahid, N. Hossain, and M. Rana, Band gap formation of 2D materials in graphene: Future prospect and challenges, *Result Eng*. **15**, 100474 (2022). https://doi.org/10.1016/j.rineng.2022.100474.
26. E. D. Obraztsova, M. G. Rybin, and P. A. Obraztsov, Optical properties of graphene, Woodhead Publishing Series in Electronic and Optical Materials, 133 (2021). https://doi.org/10.1016/B978-0-08-102848-3.00006-2.
27. S. Zhu, J. Shao, Y. Song, X. Zhao, J. Du, L. Wang, H. Wang, K. Zhang, J. Zhang, B. Yang, Investigating the surface state of graphene quantum dots, *Nanoscale* **7**(17), 7927 (2015). https://doi.org/10.1039/c5nr01178g.
28. S. Zhu, Y. Song, J. Wang, H. Wan, Y. Zhang, Y. Ning, and B. Yang, Photoluminescence mechanism in graphene quantum dots: Quantum confinement effect and surface/edge state, *Nanotoday*. **13**,10 (2017). https://doi.org/10.1016/j.nanotod.2016.12.006.

الخواص البصرية والبنيوية للأغشية الرقيقة من مركب TFB:غرافين المُحضّرة بتقنية الطلاء الدوراني

سجود باسم جبر[1] و رائد كامل جمال[1]
[1] قسم الفيزياء، كلية العلوم، جامعة بغداد، بغداد، العراق

الخلاصة

في هذه الدراسة، تمّ فحص الخواص البنيوية والبصرية للغرافين (Gr)، وبوليمر (9،9-ثنائي أوكتيل فلورين-alt-N-(4-ثانوي بوتيل فينيل)-ثنائي فينيل أمين) (TFB)، والأغشية الرقيقة المركبة من TFB:Gr المُحضّرة بتقنية الطلاء الدوراني. تمّ ترسيب الأغشية على ركائز زجاجية بسرعة دوران 1000 دورة في الدقيقة لمدة 16 ثانية، ثمّ تمّ تلدينها عند 60 درجة مئوية لمدة 30 دقيقة. تمّ فحص محاليل مركبة من TFB:Gr بنسب حجمية 5:1، 5:2، 5:3، 5:4، و5:5 لتحديد تأثير محتوى الغرافين على خواص الأغشية. أظهر تحليل حيود الأشعة السينية (XRD) أن العينة بنسبة 5:3 أظهرت قمة واضحة عند $2\theta = 26.543°$، مما يشير إلى وجود بنية الجرافين. وكشفت قياسات الامتصاص الضوئي أن زيادة نسبة الجرافين أدت إلى انخفاض فجوة الطاقة من 3 إلى 2.91 إلكترون فولت. كما أظهرت أطياف التألق تغيرات منتظمة في شدة القمة، مصحوبة بانخفاض في شدة التألق بعد دمج الجرافين في مصفوفة TFB. تُبين هذه النتائج أن التحكم في نسبة خلط TFB:Gr يوفر طريقة فعالة لضبط الخصائص البنيوية والبصرية للغشاء الرقيق المركب.

الكلمات المفتاحيه: اشباه الموصلات، البوليمرات، الخصائص التركيبية، الخصائص البصرية، الطلاء الدوراني.